Generation of high-energy soliton-like pulses in 1.9–2.5 μm spectral domain

Journal of Physics: Photonics

OPEN ACCESS

RECEIVED
14 March 2020

REVISED
5 August 2020

ACCEPTED FOR PUBLICATION
4 September 2020

PUBLISHED
1 October 2020

PAPER

Generation of high-energy soliton-like pulses in 1.9–2.5 μm spectral domain

Vladislav V Dvoyrin and Sergei K Turitsyn

Aston Institute of Photonic Technologies, Aston University, Birmingham B4 7ET, United Kingdom

Aston-Novosibirsk International Centre for Photonics, Novosibirsk State University, Novosibirsk 630090, Russia

E-mail: v.dvoyrin@aston.ac.uk

Keywords: mode-locked fiber lasers, fiber amplifiers, solitons, optical supercontinuum

Abstract

We experimentally demonstrate the generation of soliton-like pulses with 195–230 fs duration and energy up to 20 nJ in the spectral region of 1.9–2.5 μm directly from the Tm-doped all-fiber MOPA laser. The emerged Raman solitons generated directly in the fiber amplifier exhibit unusual dynamics and spectral properties forming a supercontinuum without conventional gaps between Stokes pulses. Namely, at the output powers above 2 W, in addition to conventional soliton spectral peaks beyond 2.3 μm, we observe high spectral density over an extended range of 1.95–2.23 μm corresponding to a coherent structure that to the best of our knowledge differs from any previously observed supercontinuum regimes. The average optical power of the fiber laser is at the 3-W level, whereas the estimated peak power reached the 80-kW level. Such a relatively simple laser system with high spectral density is a promising light source for various applications ranging from advanced comb spectroscopy to ultra-fast photonics.

1. Introduction

Conventional optical fibers have anomalous dispersion at wavelengths higher than approximately 1.3 μm. Nonlinear propagation of light in fiber waveguides in the main order is governed by the nonlinear Schrödinger equation (NLSE) [1], which in the case of the anomalous dispersion has well-known solutions in the form of localized coherent pulses—solitons (see, e.g. [1–3]. and references therein). Powerful enough initial waveforms of arbitrary shape (including CW radiation, as an ultimate case) during propagation down the fiber tend to transform, eventually, into soliton or set of solitons [1–3]. From a practical viewpoint, solitons have many attractive features, such as remarkable stability, a uniform phase across the pulse, and well-defined properties, e.g. pulse energy is inversely proportional to the soliton width. However, at the same time, they possess certain drawbacks, for instance, the energy of the fundamental soliton generated in the laser resonators is limited by the so-called Kelly sidebands [4]. In the case of the normal fiber dispersion it is possible to generate dissipative solitons (see e.g. [5–7]. and references therein) that can offer higher pulse energies compared to conventional solitons. However, in the red part of the spectrum (longer wavelengths), use of the normal dispersion in fibers is technically challenging.

Note, that an accurate description of the propagation of powerful and spectrally broad radiation goes beyond the NLSE model with Raman and higher-order dispersion both affecting formation of short enough pulses. Moreover, even in the limit of pure NLSE model nonstationary solutions (varying along the fiber) can be used to generate at the output new types of the localized pulse with a broad spectrum. Exploration of new forms of pulses and complex coherent structures supported by optical fibers is both an interesting scientific and an important practical problem. Of special interest is generation of structures coherent over ultra-wide spectral interval. For instance, comb spectroscopy is based on the availability of a coherent optical supercontinuum (SC) source [8, 9]. Supercontinuum can be produced in the highly nonlinear fibers through spectral broadening based on a four-wave-mixing process characterized, in general, by generation of

numerous temporal structures and de-phasing of spectral components. Even when SC consists of a set of individual solitons their relative phases might be randomly distributed (due to the underlying pseudo-random four-wave-mixing dynamics), leading in the limit of many pulses to an interesting optical phenomenon—soliton gas [10]. Typically, such SC is incoherent or quasi-coherent [8, 9] and, therefore, is not optimal for applications in the comb spectroscopy. Therefore, the study of new nonlinear mechanisms leading to formation of coherent, spectrally broad structures is of high practical interest. Here we consider an approach based on the exploiting Raman effect in an optical fiber amplifier.

Conventional applications of the Raman effect are based on the complete or almost complete transfer of energy from the pump in the shorter wavelength (blue) part of the spectrum to the longer wavelengths (red part). Thus, energy is shifting from the blue to the red part . This conventional process leads to visible spectral gaps between forming Stokes pulses. Such gaps are undesirable for many supercontinuum applications. In this work, we explore a possibility to arrange a continuous energy cascade from the blue to the red part of the spectrum, while keeping the blue part at the target level of spectral power by constant pumping in this region. This provides an opportunity to generate temporally short coherent structures with high spectral density.

A laser producing a single spectrally broadband intensive optical pulse would be highly attractive for spectral comb application. Moreover, lasers generating ultrashort broadband pulses in the mid-IR range beyond 2 μm, in particular, in the atmospheric transparency window in between 2 and 2.5 μm, are in special demand due to various practical applications. Highly intensive optical pulses are required for various applications, including micromachining and modification of material properties like inscribing of waveguides [11], LIDAR systems [12], optical coherence tomography [13], trace gas sensing [14] and others.

Tm-doped ultrafast fiber laser already overcame 100-W and 200-MW levels in average and peak powers, respectively [15, 16]; tens- and hundreds-millijoules pulse energies were demonstrated [16, 17]. Such noticeable results were obtained with bulk optics in master oscillator—power amplifier (MOPA) systems. Generation of broadband optical pulses ($\sim$1.85–2.05 μm) directly in the oscillator was also reported [18], as well as generation of spectrally tunable (1.93–2.2 μm) coherent Raman solitons in fiber amplifier [19]. However, the output average power of the fiber oscillator producing broadband pulses [18] was 20 mW, leaving room for potential further improvement, that we explore in this work. A high-power SC generation in this spectral range was demonstrated by several methods, for instance, pumping of a Ho-doped fiber amplifier with intense 1.6-μm Q-switched pulses [20], amplification of microseconds pulses from gain-switched and mode-locked Tm/Ho-doped laser in a Tm-doped amplifier [21, 22], amplification of SC generated with mode-locked or nanosecond Er-doped fiber lasers in Tm- or Tm/Ho-doped fiber amplifiers [23–29]. Generation of 25-W SC spanning from 2 to 2.5 μm has been demonstrated for a silica-based Tm-doped fibre amplifier seeded with SC produced in the result of the break-up of nanosecond pulses at 1.5 μm [30]. Pumping a specialty high-NA normal-dispersion silica fiber by Tm-doped MOPA fiber laser resulted in SC spanning from 1.77 to 2.33 μm with 92 mW of output power [31].

Generation of spectrally tunable Raman solitons and high-power mid-IR optical SC directly in straightforward all-fiber Tm-doped MOPA fiber lasers is a powerful tool for producing pulses with a substantially higher intensity and shorter duration compared to the 'parent' pulse of a seed laser [32–34]. In this work, we present new results on the application of this promising approach. We observed unusual dynamics of Raman solitons generated directly in the fiber amplifier that results in formation of a supercontinuum without characteristic gaps between conventional Stokes pulses. Namely, we observe, for the first time, to the best of our knowledge, a soliton-like structure with a high spectral density over an extended range of 1.95–2.23 μm. This process allows increasing the pulse energy through the spectral broadening, in which Raman effect transfers power to the longer wavelengths and the pumping wave compensates this migration by a new portion of incoming power without exhaustion of the shorter wavelength region. We demonstrate this new phenomenon using a relatively simple setup that makes this technique potentially promising for generation of high-power single-pulse optical supercontinuum. Such supercontinuum is highly demanded for various spectroscopic applications including advanced comb spectroscopy.

2. Methods

An all-fiber core-pumped linear-cavity SESAM-mode-locked Tm-doped silica fiber laser assembled similar to [32] is used as a pump source. The seed laser pumped by a laser diode at the wavelength of 1560 nm operates at the wavelengths of 1925 nm (figure 1(a)) with the full width at half maximum (FWHM) of 3.4 nm; the pulse duration of the seed laser is about 2 ps with the repetition rate of 69 MHz; the average output power is about 3.5 mW. The typical pulse trains observed from the seed laser and amplifier are shown in figure 1(b).

The fiber amplifier shown in figure 2 is based on a 4-m length span of a commercially available silica-based Tm-doped double-clad fiber (DCF-TM-12/128P, CorActive High-Tech Inc.). Its core and clad

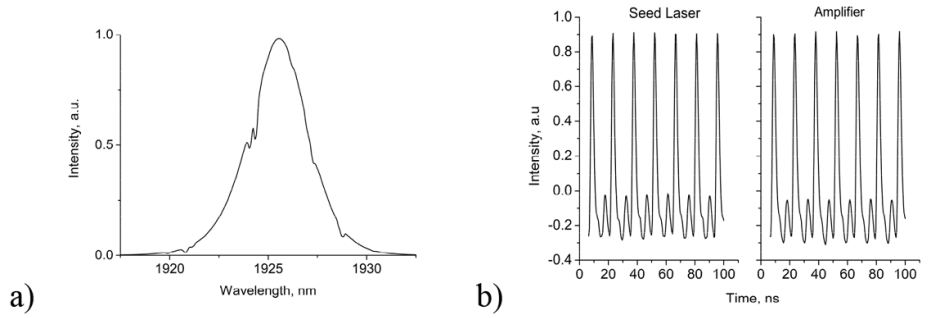

Figure 1. Optical spectrum of the seed laser (a), and typical pulse trains (b). (The smaller pulses are artefacts of measurement representing detector's response function.).

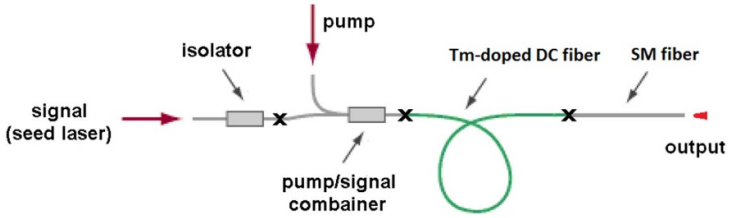

Figure 2. Scheme of the amplifier.

diameters amount to 12 and 130 μm, respectively, and its cladding cross-section is octagonal. The amplifier is clad-pumped in a forward direction by a laser diode operated at the wavelength of 793 nm. The cladding of the angle-cleaved 0.5-m span of the single-mode passive fiber (SM-2000, Thorlabs, Inc.) spliced with the amplifier output does not guide light, and the laser emission, consequently, does not contain unabsorbed pump radiation.

Pulse trains are recorded with an optical semiconductor detector (extended InGaAs) with the response time of 1 ns. Optical spectra have been observed with an optical spectrum analyzer in the wavelength domain. For readers' convenience, the frequency scale is also shown in figures representing the spectra. Power fraction corresponding to specific spectral components was calculated from the optical spectra using the knowledge about the total output optical power measured with a thermal power meter.

The interferometric autocorrelations traces were recorded with a home-made autocorrelator built using the Michelson interferometer scheme. Si or InGaAs optical detectors operating in two-photon absorption mode have been used for the detection of the autocorrelation traces. The intensity autocorrelations have been numerically restored using Fourier-filtering. The pulse durations have been calculated from the intensity autocorrelation traces under the assumption of the pulses' sech^2-profile.

3. Results

3.1. Raman solitons: optical spectra

Raman solitons have been generated directly in the amplifier. At approximately 450 mW of the total output power, a formation of a typical Raman soliton [14] was observed in the output spectra, see figure 3. The soliton holds 84% of the total energy. With pump power increase, its Raman frequency self-shift (RFSS) was observed along with the formation of an additional Raman soliton. The part of the total energy stored in the primary Raman soliton started to decrease after the formation of the second one. The average power corresponding to the first Raman soliton, however, increased reaching its maximum of 550 mW when the soliton spectral position shifted to 2.2 μm as shown in figure 3.

The spectral FWHM of the 1st Raman soliton experiencing RSFSS remained nearly constant consisting of 25 nm (1.75 THz). The side-lobes became more pronounced at higher output powers due to increased excessive energy of the soliton.

The FWHM spectrum of the 2nd Raman soliton centered near 2 μm amounted to 35 nm (2.6 THz) and was continuously rising in magnitude to $\sim$70 nm ($\sim$4.5 THz), when the soliton shifted to 2.2 μm, as illustrated by figure 4. Its spectral shape experienced deformation during RFSS; therefore, this pulse is referred to as the 2nd soliton-like pulse in what follows. Near 2 μm, the 2nd soliton-like pulse had a longer

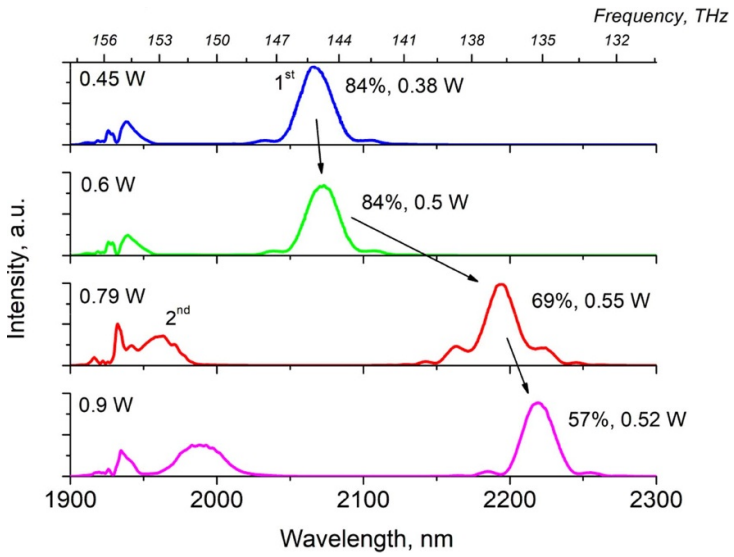

Figure 3. Output spectra for the output powers of 0.45, 0.59, 0.79, and 0.9 W.

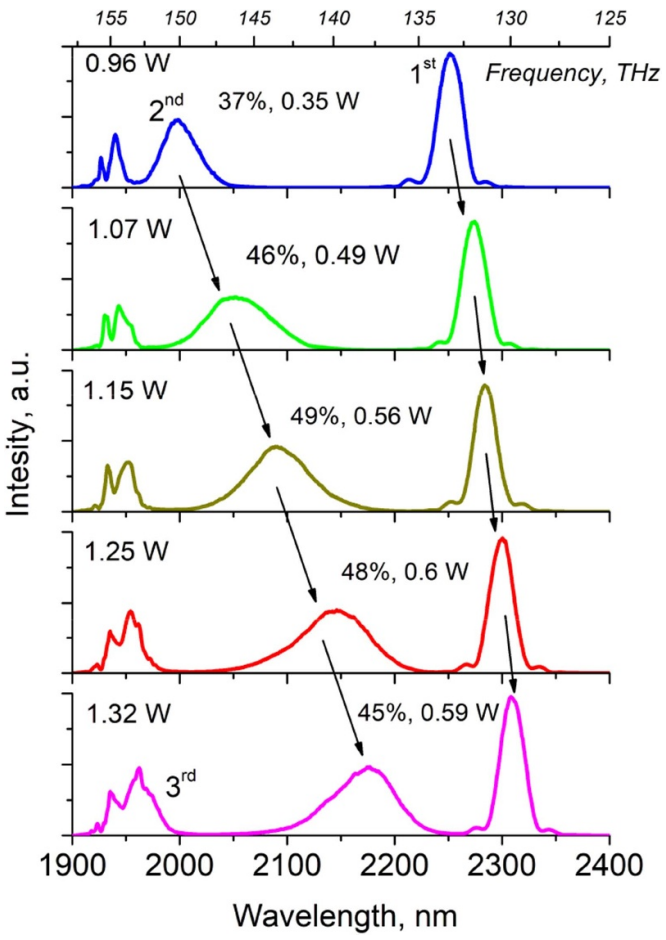

Figure 4. Output spectra for the output powers of 0.96, 1.07, 1.15, 1.25 and 1.32 W.

red wing. At around 2.15 μm it acquired an almost symmetrical shape. But near 2.2 μm (figure 5) it again distorted so that the blue wing became stronger. Simultaneously, the formation of the 3rd soliton-like pulse was noticed in the spectrum.

At the higher output power (see figure 5), RFSS of the 2nd soliton-like pulse was noticeably weaker. It took the symmetrical sech^2 shape at 1.52 W when its spectral maximum passed 2.2 μm. Its FWHM (equal to

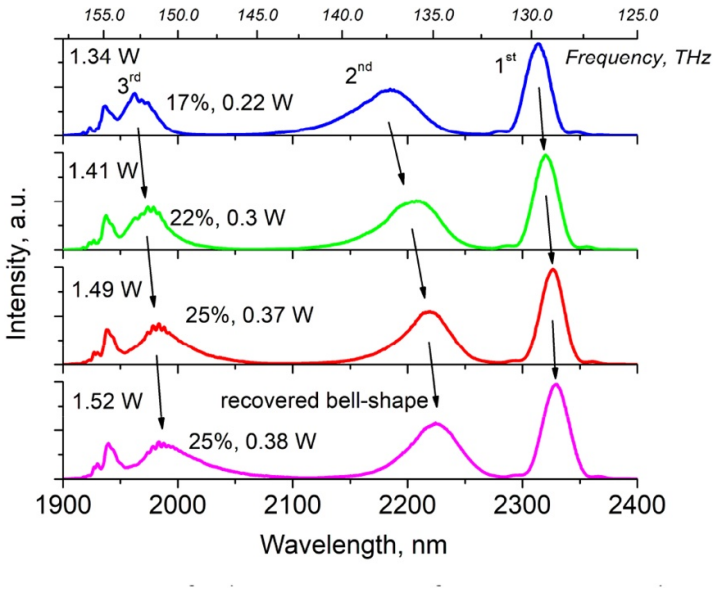

Figure 5. Output spectra for the output powers of 1.34, 1.41, 1.49, and 1.52 W.

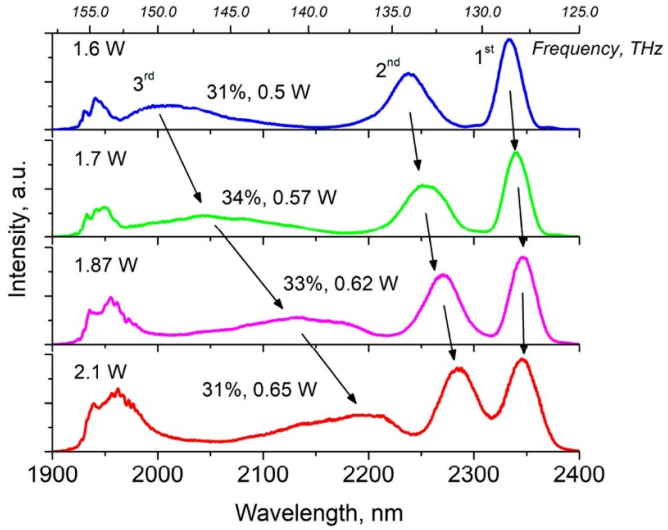

Figure 6. Output spectra for the output powers of 1.6, 1.7, 1.87, and 2.1 W.

37 nm or 2.25 THz at 1.52 W of output power) almost returned to the initial magnitude of 35 nm. The 1st Raman soliton spectral position, FWHM, and pulse energy changed insignificantly. The 3rd soliton-like pulse distinctly separated from the parent pulse.

Beyond 2.2 μm, the 2nd soliton-like pulse had the characteristic symmetric soliton-like shape (figure 6). At the same time, the changes in the parameters of the 1st Raman soliton were negligible. The 2nd soliton-like pulse experienced a stronger RFSS, and eventually both pulses noticeably overlapped in the spectral domain.

The specific spectral evolution was more pronounced for the 3rd soliton-like pulse: it had an asymmetric shape and its spectral shift was accompanied by the rise of its 'red' wing. In the vicinity of 2.2 μm, however, its 'blue' wing became stronger.

At the output power of 1.7 W, approximately, a formation of another spectral structure in the vicinity of the parent pulse was observed. Its evolution was rather different from that one expected for conventional Raman solitons experiencing RFSS. This was manifested as the strong rise of the red wing and a very weak shift of the spectral maximum. The asymmetric shape of this structure was well pronounced. At higher output powers, see figure 7, the rise of its red wing led to the formation of a continuous flat spectral profile, i.e. an optical supercontinuum. By analogy with the formation of the previous soliton-like pulses, we

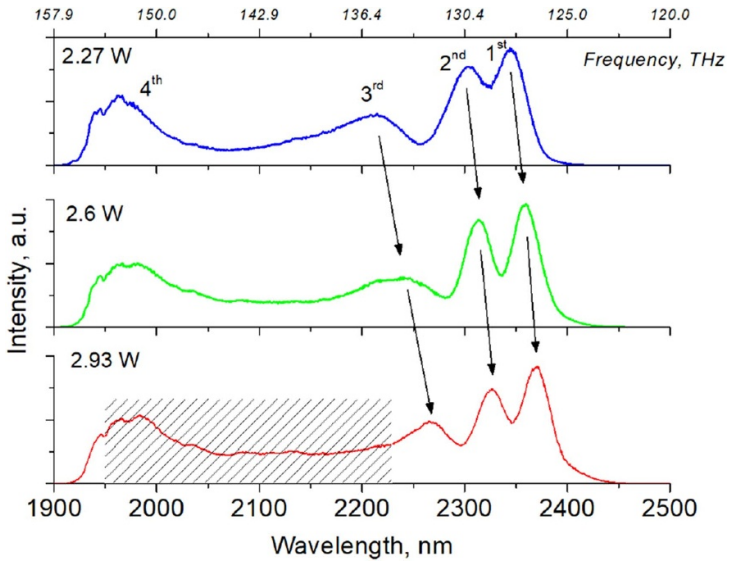

Figure 7. Output spectra for the output powers of 2.27, 2.6, and 2.93 W. The presumable area of the 4th Raman soliton at 2.93 W of the output power is hatched.

suppose that the whole spectral area shown in the dashed box in figure 7 can be mainly attributed to a femtosecond-scale pulse, which represents the main result of our work.

The FWHM of the 3rd soliton-like pulse centered at 2.29 μm at the highest output power was estimated from spectra after deduction of the spectral pedestal. It was found to be equal to approximately 40 nm (2.3 THz), i.e. comparable to other solitons. The conclusions made from the spectral analysis are supported by the study of the autocorrelation traces, which is provided in the next section.

3.2. Raman solitons: autocorrelation traces, Si detector

The autocorrelation traces have been studied neglecting the presence of the parent pulse due to its low intensity. The Si detector has a cut-off at approximately 1100 nm. The autocorrelator operated in two-photon absorption mode. Therefore, the impact of the radiation above ~2.2 μm was negligible, and it was possible to observe the autocorrelation trace of each soliton-like pulse separately, when other pulses did not exist or existed at wavelengths longer than 2.2 μm. The intensity autocorrelation traces of the pulses were well approximated by the sech^2 profile. Both interferometric and intensity autocorrelation traces of the soliton-like pulses are shown in figure 8. The traces corresponding to the 1st Raman soliton are presented in figure 8(a). The FWHM of the intensity autocorrelation was equal to 300 fs. Under the assumption of the sech^2 soliton temporal profile, the pulse duration amounted to 195 fs, which almost corresponded to the time-bandwidth limit of 190 fs. The pulse energy evaluation of 7.2 nJ from the spectra gives an estimate of the pulse peak power above the 30-kW level.

The duration of the 2nd soliton-like pulse at the output power of 1.25 W is estimated as 210 fs. This magnitude was greater than the time-bandwidth limit of ~70 fs calculated for the FWHM of 72 nm (4.65 THz) and the minimum time-bandwidth product for sech^2-shape of 0.315. Its spectral shape was asymmetric, and the interferometric autocorrelation, figure 8(b), corresponds to the typical shape of a chirped pulse. Its peak power estimated in the mentioned above way reached the 35-kW level.

The 3rd soliton-like pulse duration calculated for the output power of 1.49 W was about 220 fs being of the same magnitude as the other pulses although its asymmetric spectrum at this power was narrower, its FWHM was equal to 40 nm (3 THz). This is apparently the manifestation of a smaller chirp, which can be qualitatively observed when comparing figures 8(b) and (c). The peak power of this soliton is at a lower level of 20 kW. As this autocorrelation trace corresponds to the beginning of the pulse spectral evolution, for its energy of 5.3 nJ, greater peak power is expected at higher output powers and higher pulse energies.

Finally, the autocorrelation traces of the 4th soliton-like pulse (see figure 8(d)) recorded at the output power of 2.93 W is well approximated by a sech^2 curve, too, indicating probably that the pulse shape in the time-domain has solitonic nature, despite the fact that its spectral shape is a conventional symmetric sech^2 shape. This regime, certainly, needs further study. The autocorrelation trace of this pulse resembles typical traces of strongly chirped pulses [35–37]. The duration of this pulse obtained from the autocorrelation trace was equal to 205 fs. Because the spectral components of the pulse beyond 2.2 μm were filtered out, the pulse

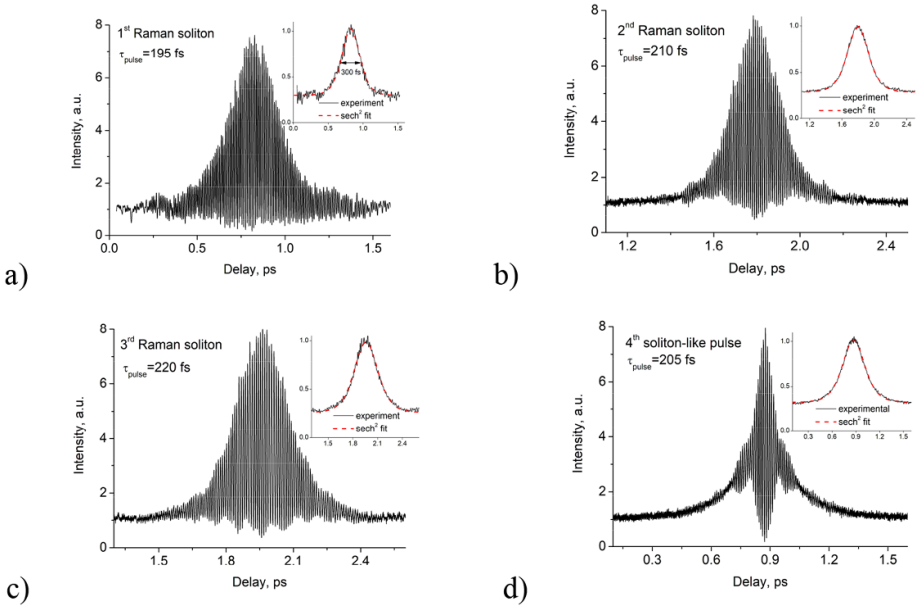

Figure 8. Interferometric and intensity autocorrelations observed at the output powers of 0.6 (a), 1.25 (b), 1.49 (c), and 2.93 (d) W.

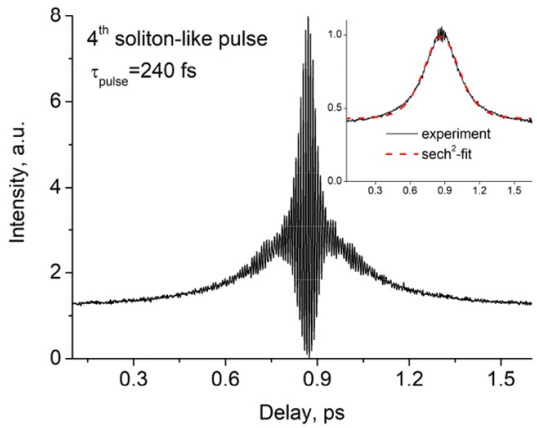

Figure 9. Interferometric and intensity autocorrelations recorded with the InGaAs detector at the output power of 2.93 W.

energy is estimated by the integration in the spectral range of 1.95–2.2 μm that gives the pulse energy estimate of 18 nJ and the corresponding peak power of 77 kW—i.e. the 80-kW peak power level.

3.3. Raman solitons: autocorrelation traces, InGaAs detector

Evidently, due to simultaneous detection of several pulses with the InGaAs detector, such traces did not allow to characterize a single pulse. However, the 4th soliton-like pulse at high output powers became noticeably stronger than others, and, we can assume that it should dominate the trace. Indeed, the intensity autocorrelation trace at the output power of 2.93 W shown in figure 9 resembles this one obtained with Si detector.

This autocorrelation trace was broader than the result recorded at the same output power with the Si detector, and the pulse duration amounted to 230 fs, which is longer than durations of other pulses obtained with Si detector. It is supposed that the spectral filtering of the strongly chirped pulse by the Si detector decreased its duration by cutting its red spectral components (back-front in time-domain). Thus, the results obtained with the InGaAs detector are believed to more adequately reflect the 4th soliton-like pulse duration. However, further more detailed studies of the fine nature of this pulse are evidently required.

The pulse energy can be estimated by cutting the spectral parts, in which other pulses (including the remains of the parent pulse) are distinctly visible. The power fraction for such region of 1.95–2.25 μm (figure 7, hatched area) corresponds to 48% of the total emission. This allows us to estimate the average

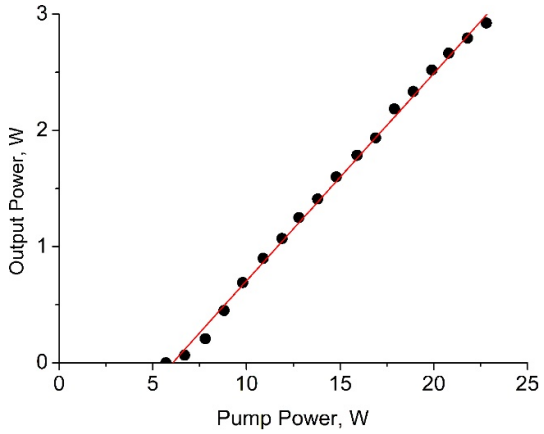

Figure 10. Output amplifier power vs. pump power.

power as 1.38 W, and the pulse energy as 20 nJ, which corresponds to 77 kW for a 230-fs pulse, or the 80-kW peak power level. This estimate shows that the pulse peak power was noticeably greater as compared to other pulses.

3.4. Energetic aspects

The dependence of the output power on the launched pump power is shown in figure 10. The maximum output power reached 2.93 W at approximately 23 W of the pump power. The amplifier slope efficiency consisted of 18%.

The maximum pulse energies are estimated from the spectra for the region of 2–2.3 μm. The maximum energy of the 1st Raman soliton consists of 8 nJ. The 2nd soliton-like pulse maximum energy was found to be higher, about 8.7 nJ. The 3rd soliton-like pulse maximum energy estimation was greater corresponding to 9.4 nJ. The already estimated last pulse energy is about 20 nJ. This pulse covered ~300-nm spectral area, and its spectrum flatness amounted to 3.6 dB in the assumption that the peaks at >2.25 μm belonged to other pulses. The minimum spectral power density was more than 3.5 mW nm^{-1} in the whole spectral range. Thus, this pulse represents itself as a good optical supercontinuum.

4. Discussion

As it has been shown in [32], in the process of soliton compression the parent pulse breaks up into several spikes giving rise to an ultrashort Raman soliton experiencing the RFSS due to its high peak power. The other pulses elongate forming eventually a long-lasting smooth pedestal. After the break-up of the parent pulse, the Raman soliton typically stores about half of the total energy. In this work, we intentionally shifted the laser wavelength at 1925 nm and used a co-propagating pump scheme in order to increase re-absorption of the remaining parent pulse. Therefore, it was possible to transfer 84% of the total output optical power into the newborn Raman soliton, as it is seen in figure 3. Strong suppression of the parent pulse in the amplifier output simplified the pattern of the autocorrelation traces eliminating multi-pulsing dynamics. This enabled analysis of the complex picture of the pulse evolution with increase the pump power of the amplifier. From the practical viewpoint, this approach will allow the development of relatively simple fiber laser source emitting ultrashort Raman solitons with a high spectral purity. The remaining fraction of the short-wavelength components can be responsible for such features of the interferometric autocorrelation traces as the non-zero minimum intensity and deviation from 1:8 of the ratio of the maximum intensity to the background. These effects exist for some traces shown in figures 8 and 9, and presumably can be explained by the presence of the short-wavelength components incoherent with the most intense pulse.

Investigation of autocorrelations of optical supercontinua has been already reported (see e.g. [38–40]. and references therein). Typically, autocorrelation traces are represented by a rather complicated structure with a broad pedestal [38–41], something that has not been observed in the present experiments. We attribute this to suppression of the contributions that affect coherence by reabsorption of corresponding spectral components in the active fiber. Spectral filtering of the optical supercontinuum allowed to reveal autocorrelation trace of its constituents (Raman solitons) [42]. However, a detailed analysis of supercontinuum structure is presented mainly by numerical simulations, e.g. [8]. The Raman solitons in our experiment are well-resolved in optical spectra, and the observed autocorrelation traces are not strongly

chirped except for the last soliton-like component. Note that a bunch of pulses with spectrally separated positions can produce an autocorrelation trace, which resembles a single chirped pulse autocorrelation. The traces obtained in our experiments are approximated well with the $sech^2$-profile. If a soliton-like structure would be, indeed, represented by a bunch of conventional solitons [25, 26, 43, 44], their durations and, therefore, their energies are expected to be comparable. This is to some extent true for the autocorrelation trace observed with the InGaAs detector. However, the maximum energy of the well-developed nearly bandwidth-limited 1st Raman soliton with 195-fs duration was equal to 8 nJ, and its FWHM was 25 nm. Therefore, a pulse with 20-nJ energy and comparable duration represented by an aggregate of pulses similar to the 1st Raman soliton should reveal its internal structure in optical spectra, i.e. a few solitons should be expressed by their individual shapes in the broad ~300-nm spectral area. Another indication of the single-pulse character of the observed soliton-like structure is that its evolution resembles the evolution of the 2nd and 3rd soliton-like pulses, which also experience spectral deformation, but tend to eventually recover their soliton spectral shape. As the deformation becomes more and more pronounced in the series of generated soliton-like pulses, it is natural to conclude that the last pulse in the series has the same nature as the previous ones. The question of its further evolution in a longer piece of a fiber or at pump power increase is open, however.

The analysis of the experimental results allows us to highlight the following specific features of the pulses' evolution.

1. The pulse evolution is gain-driven. At low pump power, the Raman soliton resembles the evolution of the conventional Raman solitons observable in the long span of optical fibers. Raman soliton experiences RFSS, its spectral shape and bandwidth are preserved well. In contrast, the shape becomes gain-dependent at high pump powers. Both active medium gain and Raman gain originated from the parent pulse can contribute to the observed spectral features.

2. The parent pulse parameters should also affect the Raman soliton evolution. Thus, several solitons emerge at high pump powers, and the evolution of earlier born solitons stronger resembles the evolution of conventional Raman solitons. The increase in the optical gain of the active medium did not visibly impact the parameters of the 1st Raman soliton except for an increase in its energy. However, when new Raman solitons appear, the state of the parent pulse (or pulses agglomerate after its break-up) is different. Apparently, this change dramatically affects the evolution of the newly produced Raman soliton. We anticipate that the Raman gain should play the key role in the observed changes in the pulses' evolution.

3. The observed pulses had a comparable duration likely originated from the mechanism of their generation. The distortion produced by subsequent amplification mainly affects their spectral broadening and chirp. Maximum pulse energy in the series of the produced pulses rises, and a new pulse becomes stronger than the previously appeared one.

4. The pulses formed after the generation of the 1st Raman soliton pulse and before the appearance of the last soliton-like pulse in the series tend to recover their soliton spectral shape. The stability of solitons against perturbations is well-known. The last pulse, however, did not show an RFSS, but rather an expansion in the longer-wavelength domain that is likely driven by the same mechanism—Raman self-amplification. We assume that its spectral expansion occurs due to Raman amplification of its long-wavelength tail by its shorter-wavelengths components. At the same time, high optical gain in the medium at these wavelengths prevents depletion of these components and compensates their extinction. Therefore, it is expected that the energy of this pulse can be further increased at higher pump powers.

We demonstrated that the parameters of the generated pulses can be manipulated and controlled in a wide range by a very simple means—increase of the amplifier pump power. This approach makes possible use of a simple picosecond seed laser to generate high-power femtosecond solitons with controlled spectral position or novel type of femtosecond soliton-like pulses with a very broad spectrum, which bandwidth can be also controlled. Such light sources are very attractive and promising for comb spectroscopy, which demands highly coherent spectrally broadband lasers.

The evolution of the seed pulse in the amplifier can be further clarified with an extension of the spectral filtering approach, which naturally occurred in our experiments due to the cut-off of the semiconductor detector. More detailed fine filtering will allow tracing the pulse evolution in the spectral domain. However, this is beyond the scope of the current work.

5. Conclusion

We presented experimental results on the proposed and developed Tm-doped MOPA fiber laser producing high-power ultrashort pulses with temporal $sech^2$-profile directly from the fiber amplifier with a low-power picosecond seed laser operating at the repetition rate of 69 MHz. The parameters of generated pulses can be easily manipulated and controlled by changing the amplifier pump power. We demonstrated the generation

of a 195-fs soliton with the peak power at the 30-kW level spectrally tunable in the range of ~2–2.4 μm, as well as a coherent soliton-like structure with the estimated duration of 230 fs, peak power at the 80-kW level, and a broad optical spectrum covering the whole range of 1.95–2.23 μm with the 3.6-dB flatness and the spectral power density >3.5 mW nm^{-1}. To the best of our knowledge, the latter type of pulse was observed for the first time. The maximum output power of the laser reached the 3-W level.

The proposed and demonstrated approach paves the way for the generation of high-power ultrashort pulses with ultra-broad spectrum directly from a fiber amplifier with a simple picosecond seed laser. This technology is attractive and promising for the development of radiation sources for various applications, including advanced comb spectroscopy.

Acknowledgments

This work was supported by the Russian Science Foundation (Grant No. 17-72-30006).

ORCID iD

Vladislav V Dvoyrin https://orcid.org/0000-0001-7358-1641

References

[1] Agrawal G P 2007 *Nonlinear Fiber Optics* 4th Ed edn (New York: Academic)
[2] Bale B, Okhotnikov O G and Turitsyn S K 2012 Modeling and technologies of ultrafast fiber lasers *In Fiber Lasers* ed O G Okhotnikov (New York: Wiley) pp 135–75
[3] Turitsyn S K, Bale B and Fedoruk M P 2012 Dispersion-managed solitons in fibre systems and lasers *Phys. Rep.* **521** 135–203
[4] Kelly S 1992 Characteristic sideband instability of periodically amplified average soliton *Electron. Lett.* **28** 806–7
[5] Vanin E V, Korytin A I, Sergeev A M, Anderson D, Lisak M and Vázquez I 1994 Dissipative optical solitons *Phys. Rev.* A **49** 2806–11
[6] Grelu P and Akhmediev N 2012 Dissipative solitons for mode-locked lasers *Nat. Photonics* **6** 84–92
[7] Chong A, Wright L G and Wise F W 2015 Ultrafast fiber lasers based on self-similar pulse evolution: a review of current progress *Rep. Prog. Phys* **78** 113901
[8] Dudley J M, Genty G and Coen S 2006 Supercontinuum generation in photonic crystal fiber *Rev. Mod. Phys.* **78** 1135
[9] Dudley J M and Taylor J R 2010 *Supercontinuum Generation in Optical Fibers* (Cambridge: Cambridge University Press)
[10] Gelash A, Agafontsev D, Zakharov V E, El G, Randoux S and Suret P 2019 Bound state soliton gas dynamics underlying the spontaneous modulational instability *Phys. Rev. Lett.* **123** 234102
[11] Ohkrimchuk A G, Mezentsev V, Dvoyrin V V, Kurkov A S, Sholokhov E M, Turitsyn S K, Shestakov A V and Bennion I 2009 Waveguide-saturable absorber fabricated by femtosecond pulses in YAG:Cr4^{+} crystal for Q-switched operation of Yb-fiber laser *Opt. Lett.* **34** 3881–3
[12] Chen Y, Räikkönen E, Kaasalainen S, Suomalainen J, Hakala T, Hyyppä J and Chen R 2010 Two-channel hyperspectral LiDAR with a supercontinuum laser source *Sensors* **10** 7057–66
[13] Courvoisier C, Mussot A, Bendoula R, Sylvestre T, Reyes J G, Tribillon G, Wacogne B, Gharbi T and Maillotte H 2004 Broadband supercontinuum in a microchip-laser-pumped conventional fiber: toward biomedical applications *Laser Phys.* **14** 507–14
[14] Sorokin E*et al* 2008 Ultrabroadband solid-state lasers in trace gas sensing *Mid-IR Coherent Sources and Applications* ed E-Z Majid and I T Sorokina NATO science series II: Mathematics, Physics and Chemistry (Berlin: Springer) pp 557–74
[15] Stutzki F *et al* 2014 152 W average power Tm-doped fiber CPA system *Opt. Lett.* **39** 4671–4
[16] Stutzki F, Gaida C, Gebhardt M, Jansen F, Jauregui C, Limpert J and Andreas T 2015 Tm-based fiber-laser system with more than 200 MW peak power *Opt. Lett.* **40** 9–12
[17] Wan P, Yang L and Liu J 2013 High pulse energy 2 μm femtosecond fiber laser *Opt. Express* **21** 1798–803
[18] Jiang J, Ruehl A, Hartl I and Fermann M E 2011 Coherent Tm-Fiber Raman-Soliton Amplifier 2011 Conference on Lasers and Electro-Optics Europe and 12th European Quantum Electronics Conference (CLEO EUROPE/EQEC) Munich, Germany Piscataway, NJ (IEEE) p CF2_4
[19] Jiang J, Ruehl A, Hartl I and Fermann M E 2011 Tunable coherent Raman soliton generation with a Tm-fiber system *CLEO:2011 - Laser Applications to Photonic Applications (Baltimore, MD, USA Piscataway, NJ)* (IEEE) p CThBB5 (https://10.1364/CLEO_SI.2011.CThBB5)
[20] Kurkov A S, Kamynin V A, Sholokhov E M and Marakulin A V 2011 Mid-IR supercontinuum generation in Ho-doped fiber amplifier *Laser Phys. Lett.* **8** 754–7
[21] Yang W Q, Zhang B, Hou J, Xiao R, Song R and Liu Z J 2013 Gain-switched and mode-locked Tm/Ho-codoped 2 μm fiber laser for mid-IR supercontinuum generation in a Tm-doped fiber amplifier *Laser Phys. Lett.* **10** 045106
[22] Tao M, Yu T, Wang Z, Chen H, Shen Y, Feng G and Ye X 2016 Super-flat supercontinuum generation from a Tm-doped fiber amplifier *Sci. Rep.* **6** 23759
[23] Yang W Q, Zhang B, Hou J, Xiao R, Song R, Jiang Z F and Liu Z J 2013 Mid-IR supercontinuum generation in Tm/Ho codoped fiber amplifier *Laser Phys. Lett.* **10** 055107
[24] Geng J, Wang Q and Jiang S 2012 High-spectral-flatness mid-infrared supercontinuum generated from a Tm-doped fiber amplifier *Appl. Opt.* **51** 834–40
[25] Swiderski J and Michalska M 2013 The generation of a broadband, spectrally flat supercontinuum extended to the mid-infrared with the use of conventional passive single-mode fibers and thulium-doped single-mode fibers pumped by 1.55 μm pulses *Laser Phys. Lett.* **10** 015106
[26] Swiderski J and Michalska M 2013 Mid-infrared supercontinuum generation in a single-mode thulium-doped fiber amplifier *Laser Phys. Lett.* **10** 035105

[27] Michalska M, Grześ P and Swiderski J 2018 8.76 W mid-infrared supercontinuum generation in a thulium doped fiber amplifier *Opt. Fiber Technol.* **43** 41–44
[28] Tarnowski K, Martynkien T, Mergo P, Sotor J and Soboń G 2019 Compact all-fiber source of coherent linearly polarized octave-spanning supercontinuum based on normal dispersion silica fiber *Sci. Rep.* **9** 12313
[29] Rampur A, Stepanenko Y, Stępniewski G, Kardaś T, Dobrakowski D, Spangenberg D-M, Feurer T, Heidt A and Klimczak M 2019 Ultra low-noise coherent supercontinuum amplification and compression below 100 fs in an all-fiber polarization-maintaining thulium fiber amplifier *Opt. Express* **27** 35041–51
[30] Alexander V V *et al* 2013 Power scalable >25 W supercontinuum laser from 2 to 2.5 μm with near-diffraction-limited beam and low output variability *Opt. Lett.* **38** 2292–4
[31] Zeng J, Akosman A E and Sander M Y 2019 Supercontinuum generation from a thulium ultrafast fiber laser in a high NA silica fiber *IEEE Photonics Technol. Lett.* **31** 1787–90
[32] Dvoyrin V V *et al* 2013 3W Raman Soliton Tunable between 2–2.2 μm in Tm-Doped Fiber MOPA Mid-Infrared Coherent Sources 2013 (Paris, France: OSA Technical Digest (online)) (Optical Society of America) p MTh1C.2
[33] Sorokina I T, Dvoyrin V V, Tolstik N and Sorokin E 2014 Mid-IR ultrashort pulsed fiber-based lasers *IEEE J. Sel. Top. Quantum Electron.* **20** 99–110
[34] Dvoyrin V and Sorokina I 2014 6.8 W all-fiber supercontinuum source at 1.9-2.5 μm *Laser Phys. Lett.* **11** 085108
[35] Reid D T, Sibbett W, Dudley J M, Barry L P, Thomsen B and Harvey J D 1998 Commercial semiconductor devices for two photon absorption autocorrelation of ultrashort light pulses *Appl. Opt.* **37** 8142–4
[36] Sorokina I T and Sorokin E 2015 Femtosecond Cr^{2+}-based lasers *IEEE J. Sel. Top. Quantum Electron.* **21** 273–91
[37] Jungkwuen A, Pyun K, Kwon O and Kim D E 2013 An autocorrelator based on a Fabry-Perot interferometer *Opt. Express* **21** 70–78
[38] Toenger S, Mäkitalo R, Ahvenjärvi J, Ryczkowski P, Närhi M, Dudley J M and Genty G 2019 Interferometric autocorrelation measurements of supercontinuum based on two-photon absorption *J. Opt. Soc. Am.* B **36** 1320–6
[39] Hooper L E, Mosley P J, Muir A C, Wadsworth W J and Knight J C 2011 Coherent supercontinuum generation in photonic crystal fiber with all-normal group velocity dispersion *Opt. Express* **19** 4902–7
[40] Sobon G, Sotor J, Przewolka A, Pasternak I, Strupinski W and Abramski K 2016 Amplification of noise-like pulses generated from a graphene-based Tm-doped all-fiber laser *Opt. Express* **24** 20359–64
[41] Sala K, Kenney-Wallace G and Hall G 1980 CW autocorrelation measurements of picosecond laser pulses *IEEE J. Quantum Electron.* **16** 990–6
[42] Farrell C, Serrels K A, Lundquist T R, Vedagarbha P and Reid D T 2012 Octave-spanning super-continuum from a silica photonic crystal fiber pumped by a 386 MHz Yb:fiber laser *Opt. Lett.* **37** 1778–80
[43] Xia C, Kumar M, Cheng M-Y, Kulkarni O P, Islam M N, Galvanauskas A, Terry F L Jr , Freeman M J, Nolan D A and Wood W A 2007 Supercontinuum generation in silica fibers by amplified nanosecond laser diode pulses *IEEE J. Sel. Top. Quantum Electron.* **13** 789–97
[44] Kumar M, Xia C, Ma X, Alexander V V, Islam M N, Terry F L Jr , Aleksoff C C, Klooster A and Davidson D 2008 Power adjustable visible supercontinuum generation using amplified nanosecond gain-switched laser diode *Opt. Express* **16** 6194–201